

# High Spatial Resolution Detection Method for Point Light Source in Scintillator

Kai Xu, Tetsuya Iizuka, Toru Nakura, Kunihiko Asada; The University of Tokyo; Tokyo, Japan

## Abstract

*Scintillation Detector has been playing an important role in radiation detection. The methods to improve the spatial resolution of scintillation detector have been widely studied. Commonly used scintillation detectors often use photon sensors attached to a scintillator to detect the position of light source in the scintillator, normally by counting the number of photons. In these cases the spatial resolution can reach about 1 mm. However some medical applications like positron emission tomography (PET) requires higher resolution. Some application-specific types of scintillation detector such as Si/CdTe Compton camera and PET crystal cube have improved the spatial resolution to about 250  $\mu\text{m}$  to 500  $\mu\text{m}$  [1]. However, the resolution of these types of scintillation detectors are mainly restricted by their hardware size. Therefore further improvement in the resolution can hardly be achieved unless the hardware has an obvious scale down. This paper introduces a method of high resolution point light source detection in scintillator by offering a scintillation detector with a new structure. Compared to the typical scintillator detector, the proposed one introduces a lightproof material with pinholes between the scintillator cube and photon sensors, which we used single-photon avalanche diodes (SPADs). Based on this novel construction the light source can be detected through photon reverse ray tracing method. The proposed scintillation detector can provide high spatial resolution about 10  $\mu\text{m}$  ~ 20  $\mu\text{m}$ , which is more than  $\times 10$  finer than the prior arts.*

## Introduction

Scintillation detector is known as an instrument for radiation detection by using the excitation effect of incident radiation on a scintillator material. The radiation will cause the scintillation phenomenon, generating a flash of photons that will pass through the transparent scintillator material. By determining the scintillation point, the incident angle of radiation can be calculated. The full width at half maximum (FWHM) of estimated scintillation position distribution is usually defined as the spatial resolution of the scintillation detector [2]. As the spatial resolution will directly affect the accuracy of the estimation for radiation incident angle, higher spacial resolution is always required especially for the medical applications like PET. The scintillation detector that PET currently uses has a very low spatial resolution. Although technologies such as new type of sensors and time of flight (TOF) [3] have been improved, the resolution of PET is still lower than other major scanning methods such as MRI.

There are two types of scintillation detectors being studied in recent years. The first type uses photon sensors directly attached to the surface of scintillator. The second type cuts the scintillator into several segments and attaches the photon sensor to each segment. The first one usually uses two kinds of photon

sensors, position-sensitive photomultiplier tubes (PS-PMTs) [4] and single photon avalanche diodes (SPADs) [5]. PS-PMTs can detect the light and provide voltage in proportion to the quantity of light. The detector reconstructs the  $x, y$  position of scintillation point from the luminous intensity distribution arriving at the cathodes of tubes. The spatial resolution is about several millimetres with the PS-PMTs whose size is 26 mm  $\times$  26 mm. SPAD is a photodetector in which a photon-generated carrier can trigger an avalanche current due to the impact ionization mechanism. This makes SPAD be able to detect low intensity signal. However SPAD cannot detect the quantity of incident light due to its nature. Therefore this type of scintillation detector usually generates SPAD data within a certain measuring time and resets the SPADs. The output data are added to estimate the position of scintillation position. In each case, this type of scintillation detector can only provide spatial resolution about 1 mm, which cannot afford the demand of medical applications like PET.

The examples for the second type of detectors are the Si/CdTe Compton Camera [6] and the PET Crystal Cube [7]. The Si/CdTe Compton Camera is composed of double-sided Si strip detectors (DSSDs) and CdTe pixel detectors. The DSSD is 400  $\mu\text{m}$  and 64 strips are implemented on each side. The spatial resolution is determined by the size and the thickness of the strip detectors and can provide 27 mm and 5 mm for the longitudinal and the lateral resolutions, respectively [8]. As the progress of research in recent years, strip detector's size has been even scaled down to several micrometers, which results in about 300  $\mu\text{m}$  spatial resolution [1]. In contrast to Si/CdTe Compton Camera, the 3D Crystal Cube (X'tal Cube) is a three-dimensional position sensitive radiation detector, composed of small crystal segment whose size is 3.0 mm  $\times$  3.0 mm  $\times$  3.0 mm with multi-pixel photon counters (MPPCs) coupled to each surface of the crystal block [7]. The spatial resolution is considered to be equal to the size of crystal block. However the spatial resolution is still not high enough for the application in PET. In addition both Si/CdTe Compton Camera and the PET Crystal Cube's spatial resolutions are restricted by their hardware size, therefore they can hardly be improved unless the hardware has an obvious scale down.

This paper proposes a method of high spatial resolution light source detection in scintillator by offering a scintillation detector with a new structure. Compared to the first type of the scintillation detector mentioned above, the proposed one introduces a light-proof material with pinholes between scintillator cube and photon sensors that are implemented with SPADs in this research. Based on this structure the light source can be detected through photon reverse ray tracing method. Simulations have been conducted to prove that this scintillation detector can provide high spatial resolution about 10  $\mu\text{m}$  ~ 20  $\mu\text{m}$ , which is more than  $\times 10$  finer than the prior arts. In addition the proposed scintillation

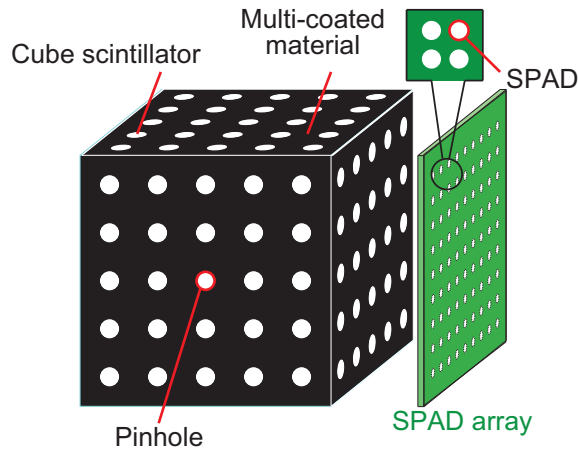


Figure 1. A structure of the proposed scintillation detector.

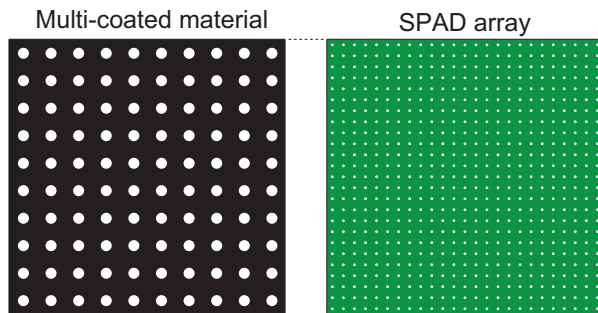


Figure 2. An example of the structure of the multi-coated material and SPAD array.

detector has a small size, which is about 1 mm ~ 10 mm for the reason that SPADs are used as the photon sensors. This small size allows the scintillation detector to be applied in various applications. One disadvantage about this scintillation detector is that the light-proof material will decrease the number of detected photons. However it offers an excellent detecting performance in terms of its high spatial resolution.

### Structure of Scintillation Detector

The structure of the proposed scintillation detector is illustrated in Figure 1. The detector is composed of a scintillator cube, multi-coated material with pinholes and SPAD array attached to each face of the cube. The multi-coated material is supposed to be completely light-proof, hence the photons generated inside the cube can pass only through the pinholes to outside of the scintillator. The SPAD arrays are attached in parallel with the face of the cube with a very narrow separation. The scintillator size is considered to be from 1 mm to 1 cm. The circular shape is assumed for both pinhole and SPAD in this research. An example of the structure of the multi-coated material and the SPAD array is shown in Figure 2. The size and the pitch of the SPADs are assumed to be smaller than those of the pinholes.

The concept of the photon detection by the proposed scintillation detector is shown in Figure 3. Supposing a gamma-ray enters the scintillator cube, with some probability it may interact

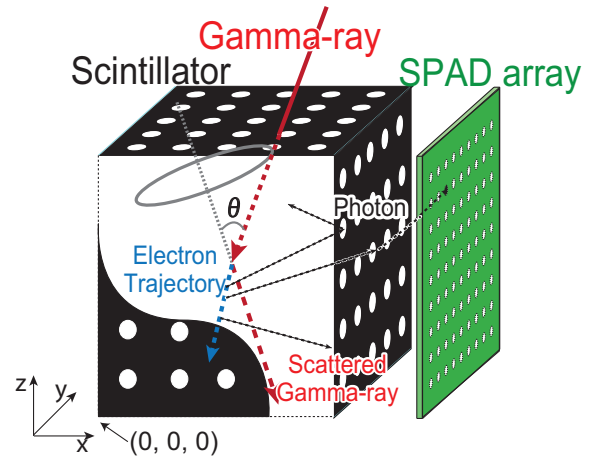


Figure 3. A conceptual diagram of photon detection with the proposed scintillation detector.

with electrons at a point in the cube to create an ionization event. The electron will move in the scintillator and the photons will be emitted along the trajectory of the electron. When the energy of gamma-ray is low, the place of interaction can be considered as a point-like isotropic radiation source [9] thus the trajectory of electron could be considered as a point [4]. A part of the emitted photons will pass through pinholes and go outside of the scintillator. Then when one of the SPADs on the array captures the photon, it will breakdown to make a pulse current, and the position of it will be read out. Although the proposed structure with light-proof material decreases the number of photons detected by the sensor thus may reduce the photon detection efficiency, the point of the scintillation event can be precisely traced back thanks to the pinhole array.

### Light Source Detection Methodology

When a photon enters a SPAD to cause breakdown, it has to come through one of the pinholes from the cube. Therefore from the photon detection results by the SPAD array, we can trace back to the point of the light emission inside the scintillator. To estimate the position of scintillation point, we need to calculate the probability distribution as a light source inside the scintillator. We consider a SPAD breakdown as a single probability event and multiple SPADs breakdown as a simultaneous event. We will introduce how to calculate the single probability event and then explain how to calculate a simultaneous event from the calculation results of single probability events.

Suppose a single SPAD breakdowns on the array, we can divide the scintillator cube into two regions: one is the region where the light source possibly exists, and the other is where that can not. The region where the light source can not exist will be ignored. By ignoring this region, the light source estimation will consume less time. Since the space between multi-coated material and the SPAD arrays is supposed to be filled with air whose refraction rate is different from the scintillator material, the calculation of the possible region is actually hard to be solved analytically. Therefore numerical calculation is chosen in this research. We assume a photon generated from the light source is captured by

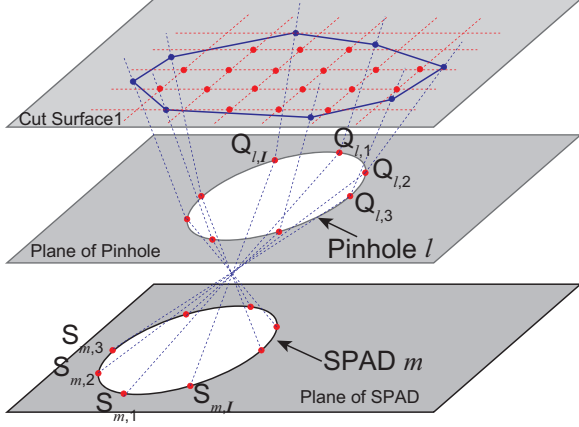


Figure 4. Calculation model of the possible light source area calculation

$m$ -th SPAD ( $I \leq m \leq M$ ,  $M$ : total number of the SPADs). The photon could possibly pass through any pinholes, therefore the possible region can be calculated using  $m$ -th SPAD and each pinhole. Figure 4 shows the calculation method for possible region using  $m$ -th SPAD and  $l$ -th pinhole ( $I \leq l \leq L$ ,  $L$ : total number of the pinholes in each surface of scintillator). The perimeter of  $m$ -th SPAD is divided equally by  $I$  points ( $S_{m,1}, S_{m,2}, \dots, S_{m,I}$ ) and that of  $l$ -th pinhole is also divided by  $I$  points ( $Q_{l,1}, Q_{l,2}, \dots, Q_{l,I}$ ) as shown in Figure 4. The  $i$ -th point ( $I \leq i \leq I$ ) on the pinhole's perimeter  $Q_{l,i}$  is assumed to be placed at the opposite side of  $S_{m,i}$  on the SPAD's perimeter. The trajectory that photon passes through the point  $Q_{l,i}$  then finally reaches the point  $S_{m,i}$  is one of the outermost edge of the possible region. Therefore the possible region is approximated by this cone-shaped region encircled by  $I$  trajectories when  $I$  is sufficiently large. The total possible region can be determined by unions of every separate possible region from  $m$ -th SPAD through each pinhole.

Since we are assuming a small cube, 1 mm on a side, the probability that an incoming gamma-ray causes a scintillation phenomenon at a point in the cube is assumed to be a constant at everywhere in the cube. Therefore, to obtain the highest possible point of light emission, we simply calculate and compare the probability that the photon emitted from the point enclosed in the cone-shaped region causes a breakdown in the  $m$ -th SPAD. We divide the scintillator cube into  $N$  lattice points and calculate the probability at each point inside the possible region. We will use  $10 \mu\text{m}$  step for a fine spatial resolution for the experiment in the next section.

The probability that a photon emitted from the  $n$ -th lattice point enters the  $m$ -th SPAD can be approximated in the following manner. As illustrated in Figure 5, the trajectory of the photon from the  $n$ -th lattice point that arrives at the point  $S_{m,i}$  on the perimeter of the  $m$ -th SPAD is assumed to go through the point  $R_{l,i}$  on the multi-coated material. Since this trajectory is one of the outermost edge of the region where the photon emitted from the  $n$ -th lattice point can enter the  $m$ -th SPAD, the photon actually can traverse to the  $m$ -th SPAD only through the area defined by the intersection between the pinhole and the shape encircled by the points  $R_{l,1}, R_{l,2}, \dots, R_{l,I}$ . The solid angle subtended by the intersection divided by the solid angle of a sphere ( $4\pi$ ) is consid-

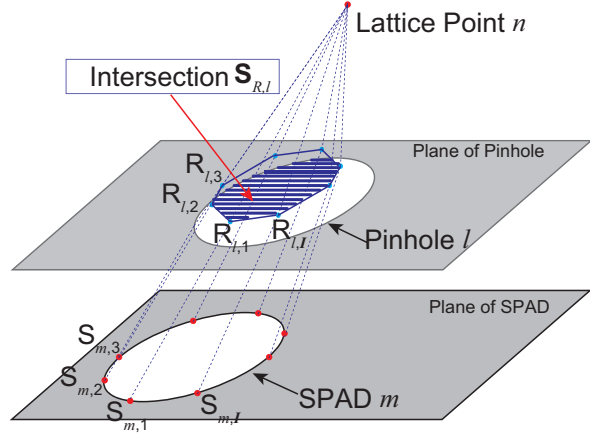


Figure 5. Calculation model of the solid angle calculation

ered to be the probability that photon emitted from the  $n$ -th lattice point enters the  $m$ -th SPAD. We define shape  $S_{R,l}$  as a shape encircled by the points  $R_{l,1}, R_{l,2}, \dots, R_{l,I}$ . The area of shape  $S_{R,l}$  is given by

$$S_{R,l} = \frac{1}{2} \left| \sum_{i=1}^I R_{l,i}(x) (R_{l,i+1}(y) - R_{l,i-1}(y)) \right|, \quad (1)$$

where we assume  $R_{l,I+1} = R_{l,0}$ , and  $R_{l,i}(x)$  and  $R_{l,i}(y)$  are the  $x$  and  $y$  coordinates of the point  $R_{l,i}$ , respectively. If  $R_{l,i}$  is outside the pinhole, then  $R_{l,i}$  in equation (1) will be replaced by  $R'_{l,m,i}$ , which is the intersection point of straight line  $R_{l,i}-O_l$  and perimeter of  $l$ -th pinhole as shown in Figure 6, where  $O_l$  is the center of the  $l$ -th pinhole. According to the parameter of our research, the interval between pinholes is large enough, thus the situation that shape  $S_{R,l}$  intersects with 2 or more pinholes can be ignored.

The solid angle  $\Omega_{n,l}$  of the intersection is approximately given by

$$\Omega_{n,l} = S_{R,l} \times \left( \frac{1}{I} \sum_{i=1}^I \cos \theta_{n,R_{l,i}} \right) \times \left( \frac{1}{I} \sum_{i=1}^I r_{n,R_{l,i}} \right)^{-2}, \quad (2)$$

where  $\theta_{n,R_{l,i}}$  and  $r_{n,R_{l,i}}$  are the photon incident angle and the distance from the  $n$ -th lattice point to the points  $R_{n,R_{l,i}}$ , respectively.

The  $\Omega_{n,l}$  divided by the solid angle of a sphere ( $4\pi$ ) is recognized as a probability  $P_m(n)$  that the  $m$ -th SPAD breakdowns due to the photon from the  $n$ -th lattice point. To make the estimation faster, we calculate the probabilities  $P_m(n)$  for every combination of SPAD  $m$  and pinhole  $n$  and save these values into a database. When these probabilities are needed to estimate the light source position, we only readout them from the database without any more calculation. The detailed flowchart of making the database is shown in Figure 7.

In an actual scintillation event multiple SPADs are supposed to breakdown therefore the probability  $P_{simul}(n)$  that multiple SPADs  $m' = 1, 2, \dots, M'$  simultaneously breakdown due to the photon from the  $n$ -th lattice point is given by

$$P_{simul}(n) = \frac{\prod_{m'=1}^{M'} P_{m'}(n)}{\sum_{n=1}^N \left( \prod_{m'=1}^{M'} P_{m'}(n) \right)}. \quad (3)$$

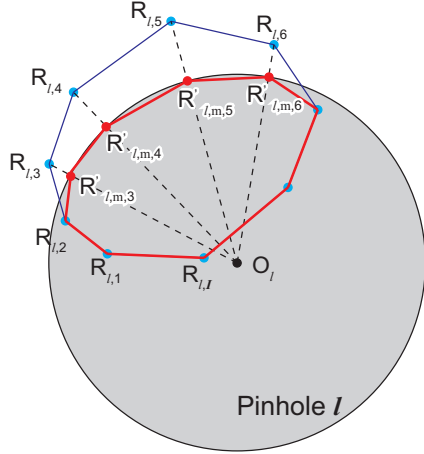


Figure 6. Calculation diagram of shape  $S_{R,l}$

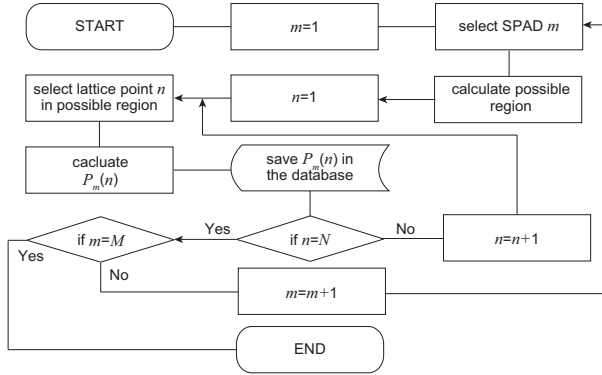


Figure 7. Flowchart of calculation of probability  $P_m(n)$  and saving probability into database

By finding the highest probability point, we can precisely detect the point of the light emission in the scintillator cube.

If we consider the SPAD implementation in reality, however equation (3) is correct only when there is no dark count in SPADs. The dark count in SPAD is defined as the count of the breakdown even without any incident light, which is mainly triggered by an undesired thermal generation [10]. Therefore in the actual implementation we have to take into account the impact of the dark count rate. When the SPAD captures no photon, there is a probability that SPAD breakdowns according to the dark count to input the wrong signal. Based on the dark count rate reported by [10], the error probability is calculated  $\sim 0.2\%$  when the time interval of measurement is assumed to be 100 ns. With this error probability, the probability  $P'_{simul}(n)$  that multiple SPADs simultaneously breakdown is now rewritten as

$$P'_{simul}(n) = \frac{\prod_{m'=1}^{M'} P'_{m'}(n)}{\sum_{n=1}^N (\prod_{m'=1}^{M'} P'_{m'}(n))}, \quad (4)$$

where

$$P'_{m'}(n) = P_{m'}(n) \times 0.998 + \frac{0.002}{N}. \quad (5)$$

The probability  $P'_{simul}(n)$  could be considered as the probability that light source is located at  $n$ -th lattice point. In the

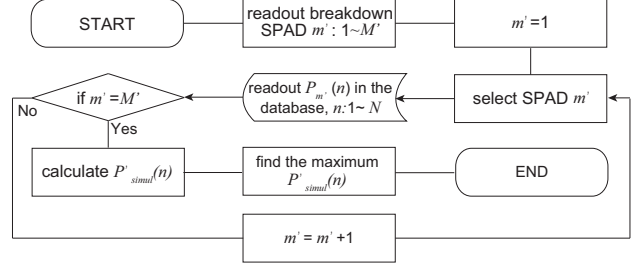


Figure 8. Flowchart of light source position estimation using the database

process to calculate probability  $P'_{simul}(n)$ , the data of probability  $P_m(n)$  is readout from the database mentioned above. The flowchart of the light source position estimation is shown in Figure 8. Probability  $P'_{simul}(n)$  will be used to detect the position of the light emission for the experimental results in the next section.

## Experimental Results

The proposed point light source detection method is implemented to demonstrate its feasibility and fine spatial resolution. The parameters of the scintillation detector structure in the experimental verification are listed in the table.  $\text{CaF}_2$  scintillator material is assumed because  $\text{CaF}_2$  is less deliquescent and has a small refractive index. The light yield is set to be 30000 photons/MeV.  $\text{Cs-137}$  is assumed to be a radiation source that emits gamma-ray of 0.662 MeV.

In the verification simulation, photons are assumed to be emitted from one point inside the scintillator in random direction by Monte Carlo method. Photons have rectilinear motion inside the scintillator and is absorbed when it hits the light-proof material. If a photon hits the pinhole, possible optical phenomenon will be (a) transmission and reflection (b) refraction and (c) diffraction. To make the simulation simpler, we assume that all photons transmit and refract at the scintillator surface without reflection, unless a total reflection phenomenon happens. If a photon is totally reflected, it will not be traced because the open rate of the pinhole and SPAD is small enough and the photon totally reflected has a very big probability to hit on the multi-coated material. The diffraction phenomenon is also ignored because the size of airy disc is small enough compared to the diameter of a SPAD here based on the simulation parameters. If a photon passes through the pinhole and finally enters the SPAD, it will breakdown with some probability. The probability, which is defined as a detection rate, is determined by SPAD photon detection efficiency. In this research, this possibility is set to be 20% based on our prior work [10]. There is a probability that the SPAD breakdowns even when there are no photons due to SPAD error rate in the previous section. The error rate due to the dark count is set to be 0.2% based on results in prior work [10].

The scintillator is placed on the horizontal plane of  $z = 0$ . Three edges of the cube are set to be  $x$ -axis,  $y$ -axis,  $z$ -axis as shown in Figure 3. The light source point is set at  $(200\mu\text{m}, 500\mu\text{m}, 700\mu\text{m})$  inside the scintillator in this experiment. In one scintillation event  $2.0 \times 10^4$  photons are emitted from the light source based on Monte Carlo method. Scintillation events have been simulated for 1,000 times. In each simulation, the probability  $P'_{simul}(n)$  of each lattice point will be calculated based on

### Parameters of proposed scintillation detector

Parameter Name	Numeric Value
Diameter of Pinhole	40 $\mu\text{m}$
Interval between Pinholes	100 $\mu\text{m}$
Diameter of SPAD	10 $\mu\text{m}$
Interval between SPADs	40 $\mu\text{m}$
Distance between SPAD and Pinhole	100 $\mu\text{m}$
Number of SPADs in a row	25
Number of Pinholes in a row	10
Scintillator size	1mm
SPAD detection rate	20%
Error rate due to dark count	0.2%

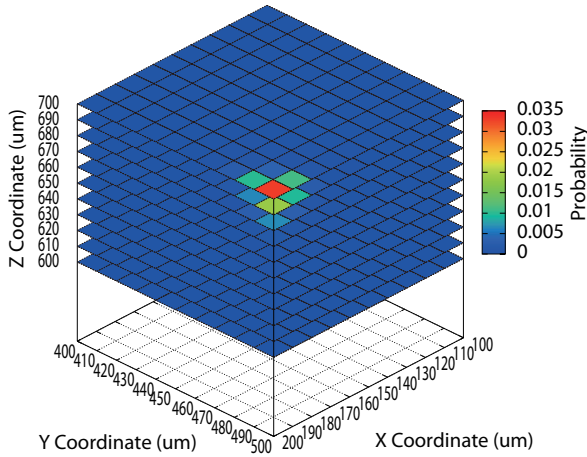


**Figure 9.**  $P'_{simul}(n)$  around the actual light source position in one scintillation event

(4). An example of  $P'_{simul}(n)$  of lattice points around light source in one scintillation event is shown in Figure 9. In this figure,  $P'_{simul}(n)$  is normalized by the sum of the probability at all lattice points. The lattice point with the highest probability  $P'_{simul}(n)$  is the coordinate (200 $\mu\text{m}$ , 500 $\mu\text{m}$ , 700 $\mu\text{m}$ ), where we set the light source.

The estimated light source coordinate is calculated in the following manner. The maximum value of  $P'_{simul}(n)$  in each  $x$ - $y$  plane is extracted. These values are normalized by their sum. Then the value is considered to be the probability at each  $z$  coordinate. Based on this method, the probability in each  $x$  coordinate and each  $y$  coordinate can also be calculated. The probability at each coordinate can be seen as a discrete probability distribution. The estimated  $x, y, z$  coordinate of light source is defined as the expected value of this probability distribution. The mean and variation values at each coordinate in 1,000 simulations are shown in Figure 10. The coordinate with the highest probability is the set position according to Figure 10.

To evaluate the spatial resolution of the proposed scintillation detector, 1,000 simulations are conducted and the histograms of the results are shown in Figure 11. The spatial resolution which is defined with FWHM is 14  $\mu\text{m}$ , 6  $\mu\text{m}$  and 7  $\mu\text{m}$  for  $x$ ,  $y$  and  $z$  coordinate. The spatial resolution is different among these  $x$ ,  $y$ , and  $z$  coordinates because the spatial resolution is affected by the exact value of each coordinate. From the simulation results of

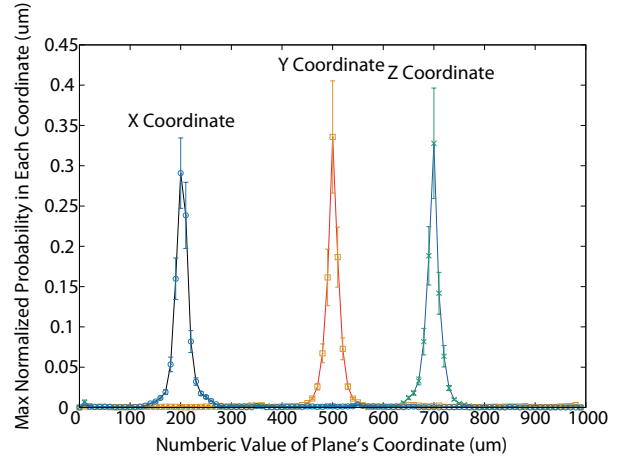


**Figure 10.** Mean and variation probability of light source in each coordinate in 1,000 simulations when light source is placed at (200 $\mu\text{m}$ , 500 $\mu\text{m}$ , 700 $\mu\text{m}$ ) inside the scintillator cube

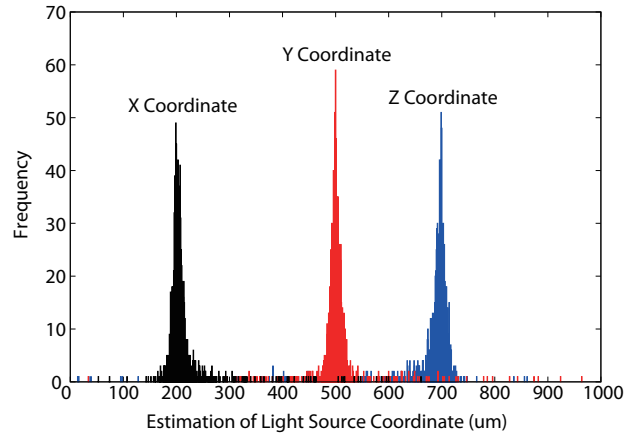


**Figure 11.** Histograms of light source coordinate estimation based on the proposed scintillation detector in 1,000 simulations

several light sources in different positions inside the scintillator, it is concluded that the proposed scintillation detector using photon reverse ray tracing method can provide a spatial resolution about 10  $\mu\text{m}$  ~ 20  $\mu\text{m}$  in this construction. As shown in Figure 11, there is a little probability that the estimated light source position has more than 100  $\mu\text{m}$  error. This is because the number of breakdown SPADs is not enough for an accurate estimation. When we increase the number of emitted photons or increase the SPAD photon detection efficiency, the error decreases rapidly.

To highlight the advantage of the proposed detection method by comparing with the conventional luminous intensity distribution method, an imaginary sensor that has the same size as a SPAD and the same photon counting capability as a PS-PMT is assumed. This imaginary sensor does not exist in reality. However we assume it because it is convenient to demonstrate the advantages of the proposed detection method. In this simulation the light source is again placed at (200 $\mu\text{m}$ , 500 $\mu\text{m}$ , 700 $\mu\text{m}$ ) inside the scintillator with the same parameters in the previous experiment. In this case with the imaginary sensor, the lightproof material is removed. Under an ideal situation where the imaginary sensor has 100% de-

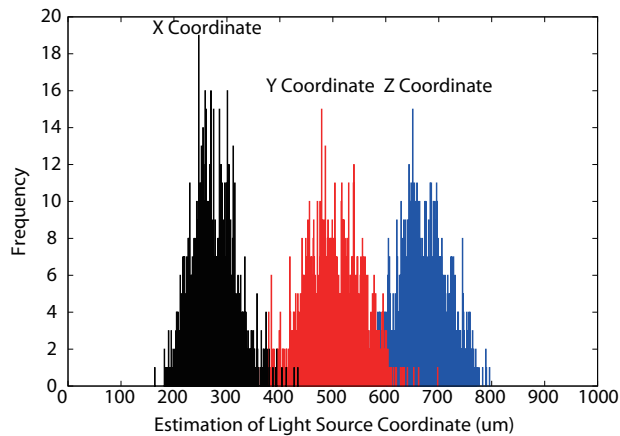


**Figure 12.** Histograms of light source coordinate estimation with imaginary ideal photon sensors by the conventional luminous intensity distribution

tection rate and no noise, we have done 1,000 simulations. Light source position are calculated based on the luminous intensity distribution method [4]. The luminous intensity is defined as a sum of voltage output of  $5 \times 5$  sensors around the corresponding sensor. Since the area of sensor arrays in this research is considered to be limited, the estimated coordinate is provided by calculating the mean of luminous intensity in each position that has luminous intensity larger than the maximum luminous intensity  $\times 0.8$ . The histogram of the estimated  $x$ ,  $y$  and  $z$  coordinates in 1,000 simulations are shown in Figure 12. The spatial resolution in this case is about  $100 \mu\text{m}$ , which is about  $\times 10$  times' bigger than the proposed photon reverse ray tracing method. This result proves that the proposed detection method fundamentally realizes finer resolution.

## Conclusion

This paper proposed a new scintillation detector with a light-proof material between the scintillator cube and the photon sensors. Although the pinholes on the light-proof material decrease the number of photons captured by the sensor, they restrict the light source position so that the light source in scintillator is calculated mathematically using the photon reverse ray tracing method. The simulation results demonstrated that the proposed scintillation detector offers a fine spatial resolution of about  $10 \mu\text{m} \sim 20 \mu\text{m}$  considering the practical parameters and non-idealities such as the number of emitted photons, SPAD photon detection efficiency and its dark count rate. The fundamental improvement of the spatial resolution with the proposed structure was proved by the comparison with the conventional luminous intensity distribution method.

## References

- [1] S.Watanabe *et al.*, "High Energy Resolution Hard X-Ray and Gamma-Ray Imagers Using CdTe Diode Devices", *IEEE Trans. Nucl. Sci.*, Vol.56, No.3, Jun. 2009.
- [2] J. Kataoka *et al.*, "Nuclear Instruments & Methods in Physics Research A (2014)," <http://dx.doi.org/10.1016/j.nima.2014.11.004>
- [3] L. Cosentino *et al.*, "Time and DOI Resolution Measurements of Minidetectors for a PET-TOF Prostate Probe", *IEEE Nuclear Science Symposium Conference Record* 2011.

- [4] N. Uhlmann *et al.*, "3D-Position-Sensitive Compact Scintillation Detector as Absorber for a Compton-Camera", *IEEE Trans. Nucl. Sci.*, Vol. 52, No.3, Jun. 2005.
- [5] A. C. Therrien *et al.*, "Modeling of Single Photon Avalanche Diode Array Detectors for PET Applications", *IEEE Nuclear Science Symposium Conference Record*, 2011.
- [6] S. Watanabe *et al.*, "A Si/CdTe Semiconductor Compton Camera", *IEEE Trans. Nucl. Sci.*, Vol. 52, No.5, Oct. 2005.
- [7] Y. Yazaki *et al.*, "Development of the X'tal Cube : A 3D Position-Sensitive Radiation Detector With All-Surface MPPC Readout," *IEEE Trans. Nucl. Sci.*, Vol.59, No.2, Apr. 2012.
- [8] M. Yamaguchi *et al.*, "Spatial Resolution of Multi-Head Si/CdTe Compton Camera for Medical Application", *IEEE Nuclear Science Symposium Conference Record*, 2009.
- [9] J. Gál *et al.*, "Theoretical study of three-dimensionally position-sensitive scintillation detector based on continuous crystal", Institute of Nuclear Research of the Hungarian Academy of Sciences, P. O. Box 51, H-4001 Debrecen, Hungary.
- [10] X. Yang *et al.*, "A  $15 \times 15$  single photon avalanche diode sensor featuring breakdown pixels extraction architecture for efficient data readout", *Japanese Journal of Applied Physics* 55, 04EF04(2016).

## Author Biography

Kai Xu was born in Shandong province, China, on May 21, 1991. He received the B.S. degree in electronic engineering from the University of Tokyo in 2015. He is currently pursuing the M.S. degree in electronic engineering at the University of Tokyo. His current research interests include architecture of scintillation detector and data analysis.

Tetsuya Iizuka received the B.S., M.S., and Ph.D. degrees in electronic engineering from the University of Tokyo, Tokyo, Japan, in 2002, 2004, and 2007, respectively. He is currently an Associate Professor with VLSI Design and Education Center (VDEC). From 2013 to 2015, he was a Visiting Scholar with University of California, Los Angeles, CA, USA. His current research interests include data conversion techniques, high-speed analog integrated circuits, digitally-assisted analog circuits and VLSI computer-aided design.

Toru Nakura received the B.S. and M.S. degrees in electronic engineering from The University of Tokyo, Tokyo, Japan, in 1995 and 1997 respectively. Then he worked as a high-speed communication circuit designer using SOI devices for two years, and worked as a EDA tool developer for three years. He joined the University of Tokyo again as a Ph.D. student in 2002, and received the degree in 2005. After two years industrial working period, he is now an associate professor at VLSI Design and Education Center (VDEC), The University of Tokyo. His current interest includes signal integrity, reliability and digitally-assisted analog circuits.

Kumihiro Asada received the B.S., M.S., and Ph.D. degrees in electronic engineering from the University of Tokyo, Tokyo, Japan, in 1975, 1977, and 1980, respectively. He joined the Faculty of Engineering, University of Tokyo, in 1980, and became a Lecturer, an Associate Professor, and a Professor in 1981, 1985, and 1995, respectively. From 1985 to 1986, he was with the University of Edinburgh, Edinburgh, U.K., as a Visiting Scholar supported by the British Council. In 1996, he established the VLSI Design and Education Center (VDEC), with his colleagues in the University of Tokyo, which is the center to promote education and research of VLSI design in all the universities and colleges in Japan. He is currently in charge of the Director of VDEC. His current research interests include design and evaluation of integrated systems and component devices.